Journal of Materials Chemistry C

Lead Halide Perovskite Quantum Dots for Light-Emitting Devices

Journal:	*Journal of Materials Chemistry C*
Manuscript ID	TC-REV-07-2018-003561.R1
Article Type:	Review Article
Date Submitted by the Author:	22-Aug-2018
Complete List of Authors:	Chiba, Takayuki; Yamagata University, Graduate School of Organic Materials Science Kido, Junji; Yamagata University, Graduate School of Organic Materials Science

Lead Halide Perovskite Quantum Dots for Light-Emitting Devices

*Takayuki Chiba** *and Junji Kido*

Graduate School of Organic Materials Science, Research Center for Organic Materials, Frontier Center for Organic Materials, Yamagata University, 4-3-16 Jonan, Yonezawa, Yamagata 992-8510, Japan

*Corresponding authors.
E-mail: T-chiba@yz.yamagata-u.ac.jp
Tel. & Fax: +81-238-26-3595

Abstract

Lead halide perovskites (LHP) have progress in not only photovoltaic materials but also light-emitting materials in recent years. In particular, nano-sized LHP quantum dots (QDs) have attracted much attention as good candidates for display and lighting application due to their excellent optical properties such as narrow emission, high photoluminescent, and color tunability. In this review, we discuss the current approaches to achieve highly efficient LHP-QDs based LEDs. We focus on the four categories, (i) synthesis and optical characterization, (ii) purification process, (iii) ligand exchange for surface passivation, and (iv) blue and red LHP-QDs LEDs.

1. Introduction

Lead halide perovskites (LHPs) have a ternary component crystal structure, $APbX_3$, where A is a cation site and X is a halide site ($X = Cl^-$, Br^-, or I^-), which are classified two types; the former hybrid organic-inorganic LHPs using organic alkyl cation such as methylammonium or formamide[1-6] and the later all inorganic LHPs using metal cation such as cesium (Cs^+)[7-9] in A-site of perovskite structure. Hybrid organic-inorganic LHPs $MAPbX_3$ bulk films have both a strong absorption coefficients and small exciton binding energy, which lead to highly efficient photovoltaics (PVs) materials with power conversion efficiency up to 20% in recent several years.[10-12] On the other hand, LHPs have attracted much attention for applications in not only PVs, but also light-emitting devices (LEDs) due to their high color purity emission spectra with narrow full width at half maximum (FWHM) and low-cast solution processed semiconducting materials. Early research on LHPs based LEDs have been attempted in 1990s, however, electroluminescence (EL) spectra could not be observed at room temperature, but it exhibited at only liquid nitrogen temperature.[13] First reported hybrid organic-inorganic LHPs based LEDs exhibited a bright EL with external quantum efficiency (EQE) of 0.73% at room temperature in 2014.[1] Subsequently, grain

size[2], interfacial engineering controls[14], quasi-two-dimensional Ruddlesden–Popper-type perovskites[15-18] have been developed to achieve high efficiency LHPs based LEDs, which reached an EQE of 14.3%[17] and 16.3%[19] for green emission, and an EQE of over 10% for red emission hybrid organic-inorganic LHPs based LEDs[14, 20] within over the past years.

All inorganic LHPs with $CsPbX_3$ have been demonstrated a novel classified colloidal light-emitting quantum dots (QDs), which have also expected great potential for the application in LEDs due to their superior chemical stability, narrow emission spectra enable coverage the next generation of standard for display, B.T. 2020 color gamut, high photoluminescence quantum yields (PLQYs) of up to 90%, plainly tunable emission wavelength in full visible range by halide anion composition (X site = Cl^- for blue emission, Br^- for green emission, or I^- for red emission) or size of QDs.[21-30] All inorganic $CsPbX_3$ LHP-QDs were synthesized by the hot-injection method in 2015.[21] The EQE of LEDs based on $CsPbX_3$ LHP-QDs have rapidly increased from 0.1% to over 8% for past only three years, although there are several issues such as unestablished purification process, ligand desorption, surface defect, insulating behavior of surface ligand, and poor stability of LEDs. In this review, we focus on current progress of LHP-QD based LEDs, issue and challenge for high efficiency and high stability LEDs.

2. Synthesis and characterization of perovskite QDs

Protesescu et al. reported that the development of novel hot-injection synthesis method for colloidal all inorganic $CsPbX_3$ LHP-QDs using lead halides (PbX_2, where X is Cl, Br, or I) and cesium-oleate precursors.[21] These LHP-QDs are ionic nanocrystal materials with cubic crystal shape and phase at room temperature, which result in a relative lower reaction temperature (below 200 ˚C), fast reaction time (only few seconds), and narrow size distributions compared to the hot injection with traditional Cd based QDs (over 200 ˚C and few minutes) (Fig. 1 a-c).[31] The size of LHP-QDs can be controlled in the range of 4–15 nm by reaction temperature and reaction time. Another synthesis route of LHP-QDs, room temperature ligand-assisted reprecipitation (LARP) method[32-36] and microwave assisted synthesis[37-39] have also been reported. LHP-QDs have a size dependency of optical properties, which exhibits tunable both optical band gap and emission wavelength by QDs diameters that smaller size lead to wide energy gap and blue shift due to the quantum size effect, whereas larger size of QDs exhibit a narrow gap and red shift of emission.[40, 41] In addition, the chemical composition of halide X-site can be drastically tuned band gap and emission wavelength in the range of ultraviolet to near-infrared region; 410 nm for $CsPbCl_3$, 510 nm for $CsPbBr_3$, and 700 nm for $CsPbI_3$. The photoluminescence (PL) spectra of LHP-QDs exhibit broader FWHM as increasing wavelength from 12 nm ($CsPbCl_3$) to 40 nm ($CsPbI_3$) corresponding to less than 100 meV, remarkable high PLQY of up to 90%, and fast PL lifetime of less than 30 ns (Fig. 1d). In addition, the toxicity of heavy metal component “lead (Pb)” in LHP-QDs is unestablished issue for

application.[42-49] The current limit the use of Pb is 1000 ppm by weight in electric application from the European Restriction on Hazardous Substances (RoHS), which is more permissive than that of Cd (100 ppm by weight). Therefore, lead-free perovskite QDs have been demonstrated using tin (Sn)[43, 44], antimony (Sb)[47], and bismuth (Bi)[48, 49], unfortunately lead-free perovskite QDs exhibited a weak PL emission with large FWHM at room temperature so far.

In order to impart both dispersibility in non-polar organic solvents (toluene, hexane, or octane) and precis size control, long alkyl oleic acid (OA) and oleylamine (OAM) were generally used as surface ligands on LHP-QDs. Colloidal LHP-QDs dispersion in non-polar solvent can be easily form a smooth thin-film by solution processing such as spin coating for the LEDs fabrication with low cost, large area, and flexible characteristics as well as the use of established fluorescent or phosphorescent small molecules, polymers and Cd-based QDs. The valence band and conduction band of LHPs are located close to the highest occupied molecular orbital (HOMO) and lowest unoccupied molecular orbital (LUMO) of typical organic light-emitting semiconductors used in organic light-emitting devices (OLEDs). Therefore, LHP-QDs can be applied the established OLED structures, which enable the effective charge injection from neighboring charge transport or electrodes. By contrast, traditional Cd based QDs with wide gap outer shell (ZnS) has a deep The valence band, which result in high charge injection barriers from neighboring layers to QDs layers.[50-52]

Song et al. reported all inorganic LHP-QD based LEDs with blue ($CsPb(Cl/Br)_3$), green ($CsPbBr_3$), and orange ($CsPb(Br/I)_3$) LHP-QDs for the first time.[53] In general, poly(3,4-ethylenedioxythiophene):poly(styrenesulfonate) (PEDOT:PSS) is used as hole injection layer, and poly(4-butylphenyl-diphenyl-amine) (poly-TPD), poly(9,9-dioctyl-fluorene-*co*-*N*-(4-butylphenyl)-diphenylamine) (TFB), or poly(9-vinylcarbazole) (PVK) are used as hole transport layer in standard LHP-QD based LEDs structure (Fig. 1e). *Tris*-(1-phenyl-1H-benzimidazole) (TPBi) is used as electron injection layer. The EL peak wavelength of blue, green, and orange LHP-QD based LEDs were 455, 516, and 587 nm with narrow FWHM of 20, 23, and 23 nm, respectively. The peak luminance and EQE were 742 cd/m^2 and 0.07% for $CsPb(Cl/Br)_3$, 946 cd/m^2 and 0.12% for $CsPbBr_3$, 528 cd/m^2 and 0.09% for $CsPb(Br/I)_3$ (Fig. 1e), which demonstrated that the use of LHP-QDs in LEDs as light-emitting materials have attracted attention for display and lighting applications as well as organic compounds or Cd-based QDs.

3. Purification process of perovskite QDs

The purification process of LHP-QDs is still unestablished, which result in a lower efficiency of LHP-QDs based LED compared to the OLED and Cs-based QD LEDs. Generally, the reprecipitation methods have demonstrated for the purification of LHP-QDs because synthesized

crude solution contains impurities such as reaction solvent octadecene and ligand precursors OA or OAM (Fig. 2a). These impurities are electrical insulating that inhibits a charge injection or transport in the LHP-QD based LEDs. Long alkyl ligands capped LHP-QDs were dispersive in non-polar solvent with low dielectric constant, e.g. toluene, octane, and hexane, which act as good solvent in reprecipitation process, whereas the polar solvents with high dielectric constant such as alcohols and ketone solvents have play a role in poor solvent.[54] When the poor solvents added to LHP-QDs dispersion in good solvent, which allow for precipitation and isolation of LHP-QDs by centrifugation. The impurity containing supernatant was discarded to removal of impurities that were soluble in polar solvents. Their long alkyl ligands OA and OAM were weak bonding to the surface on LHP-QDs, which cause an easily ligand desorption and colloidal instability during the reprecipitation process.[55, 56] In addition, ionic feature of LHP-QDs were enormously sensitive to polarity of solvents. For instance, high dielectric constant alcohols such as methanol (ε = 33.1), ethanol (ε = 23.8), and isopropanol (ε = 20.1) were used of poor solvent for reprecipitation of LHP-QDs, which cause an optical quenching due to easily decomposition of perovskite structure.[57] Therefore, purification and isolation of LHP-QDs are more difficult to handle compared with the case of typical Cd-based QDs reprecipitation. Appropriate choice of poor solvents with moderate dielectric constant (ε < 10) and increasing reprecipitation cycle are significantly important for effective purification of LHP-QDs.[58]

The systematic purification process of $CsPbBr_3$ QDs for achieving high efficiency LEDs was reported by Li et al. that multicycle reprecipitation using low dielectric constant poor solvent ethyl acetate (ε = 6.02).[59] The use of ethyl acetate as a poor solvent enables a multicycle reprecipitation due to controlling the ligand desorption on the $CsPbBr_3$ QDs. The presence of impurities was confirmed by proton nuclear magnetic resonance (^{1}H-NMR) measurement. In the case of one reprecipitation cycle sample was not sufficient purification because terminal alkene resonace in reaction solvent octadecene is observed at 4.9 and 5.8 ppm. As increasing number of reprecipitation cycle, these resonance peaks were disappeared, which demonstrate that the fully removal of octadecene. The estimated ligand density of $CsPbBr_3$ LHP-QDs surface was 6.7 nm^{-2} for one-cycle, 4.8 nm^{-2} for two-cycle, and 3.9 nm^{-2} for three-cycle, respectively (Fig. 2b, c). These results suggest that multi reprecipitation cycles could be not only removed impurity octadecene but also adjusted surface ligand density. The green LED based on two-cycle reprecipitation $CsPbBr_3$ QDs reached the peak EQE of over 6% with high luminance of over 15,000 cd/m^2 (Fig. 2d).

4. Surface passivation for perovskite QD LEDs

In order to resolve various issues such as colloidal instability in dispersion, aggregation in film, chemical decomposition, and, phase transformation, surface passivation strategy of LHP-QDs has been demonstrated that are categorized into four-approaches, additional passivation layer, ligand

exchange via post-treatment, ligand replacement via hot-injection method, and halide-rich composition synthetic method. The chemical structure of conventional long alkyl ligands, surface passivation materials, and effective surface ligands are listed in Fig. 3.

PLQYs of LHP-QDs in film were typically lower value of approximately 30%, which was drastically decreased compared with PLQYs in colloidal dispersion (ca. 80%). One of the reason this result is derived from closed packed LHP-QDs that facilitated an optical quenching by non-radiative energy transfer.[60] Thus, additional passivation layer with LHP-QDs was developed using trimethylaluminum (TMA) vapor treatment.[60] The LHP-QDs coated with TMA can be form insoluble film due to the effect of crosslinking adjacent each LHP-QDs that is derived from the hydrolysis of TMA by expose ambient air condition. This crosslinking approach allows the multilayer structures that adjacent charge injection or transport layer can be coating onto insoluble LHP-QD film by solution processing. Moreover, PLQY of $CsPbBr_3$ and $CsPbI_3$ LHP-QD films drastically increased with increasing TMA vapor treatment time (0 to 10 second), from 35% in the untreated $CsPbBr_3$ film to 60% in $CsPbBr_3$ with TMA film and 20% in the untreated $CsPbI_3$ film to 80% in $CsPbI_3$ with TMA film at reaction time of only 2 sec, respectively. This result suggested that TMA treatment enable passivation of surface defects on LHP-QDs and improvement PLQYs.

Polyhedral oligomeric silsesquioxane (POSS), cagelike structure containing siloxane core with organic corner substituent group was also demonstrated as beneficial passivation layer.[61] POSS coated LEDP-QDs improved their water or poor solvent resistivity, and film forming ability. The LED based on additional POSS layer exhibited EQE of 0.35%, which was 17-fold enhancement to control device without POSS. In addition, luminance and operational stability of LEDs with POSS layer were also improved compared to the LED without POSS, which indicating the hole-blocking effect of POSS.

As the next approach, ligand exchange process via simple two-step reaction in dispersion has demonstrated to achieve surface passivation, high PLQYs, and high efficiency LEDs. Di-dodecyl dimethyl ammonium bromide (DDAB) consists of relative shorter alkyl chain (C12) with halide ion pair that lead to facilitate both charge injection or transport and effective surface passivation in LHP-QDs.[57, 62, 63] In this process, small amount of OA was added into purified $CsPbBr_3$ LHP-QDs dispersion to desorb OAM from LHP-QD surface (first step), subsequently DDAB solution in toluene was quickly injected into mixture dispersion under stirring (second step) (Fig. 4a). Ligand exchange $CsPbBr_3$-DDAB is higher PLQY of 71% with high colloidal stability than those of pristine $CsPbBr_3$ with OA and OAM (49%) due to better surface passivation, although peak emission wavelength and size of particle is almost identical during two-step ligand exchange process. The green LED based on ligand exchange $CsPbBr_3$-DDAB exhibited a maximum luminance of 330 cd/m^2 and peak EQE of 3.0%, which was significantly higher than the LED without ligand exchange pristine $CsPbBr_3$ with OA and OAM.[63] Furthermore, the combination

ligand exchange and purification process was further effective for greater LED efficiencies. The DDAB-capped $CsPbBr_3$ with butyl acetate ($\varepsilon = 5.01$) two-wash exhibited high PLQYs of 42% even in film. The LED based on $CsPbBr_3$-DDAB purified by butyl acetate was achieving a low turn-on voltage of only 2.6 V and high EQE of 8.7%.[57] Recently, Song et al have reported on a room-temperature synthesis method for $CsPbBr_3$ QDs with triple-ligand surface engineering strategy.[64] The use of tetraoctylammonium bromide (TOAB), octanoic acid (OTAc), and DDAB result in a high ink stability, high PLQY and single exponential PL decay. The short alkyl OTAc is also effective for charge injection and transport properties in thin film. Moreover, the addition of organic cation such as formamidinium (FA) increased PLQY of 61% due to reduce surface defect by A-site engineering. The green LED based on FA doped $CsPbBr_3$ QDs exhibited remarkable high EQE of 11.6%. Therefore, mix cation engineering in A-site is also significantly strategy to achieve high efficiency of LHP-QD LEDs.

The replacement of typical long alkyl ligand OA and OAM by octylphosphonic acid (OPA) with shorter alkyl chain (C8) by direct hot-injection synthesis have recently reported.[65] The interaction between LHP-QDs and OPA was strong that allowed a multi reprecipitation cycles using methyl acetate even when eight-times due to retained high ligand density. Thus, PLQYs was kept after eight-times reprecipitation and improved PL stability (Fig. 4b). The $CsPbBr_3$ capped with OPA based LED exhibited a high EQE of 6.5%, which was 8-fold improvement compared with typical OA and OAM ligand based LEDs (0.85%). Another ligand capping strategy, zwitterionic long alkyl chain with deprotonated acid and quaternary ammonium such as sulfobetaines, phosphocholines, and γ-amino acids have been demonstrated to simultaneously achieve high colloidal stability and high PLQYs (Fig. 4c).[66] These zwitterionic ligands results in tightly coordinated with perovskite QD surface compared to the conventional OA and OAM. Thus, optical properties (PL, PLQY, and PL-lifetime) of zwitterionic-capped $CsPbBr_3$ maintained after reprecipitation washing process and long-term storage stability. The sulfobetaine-capped $CsPbBr_3$ based LEDs exhibited a peak EQE of 2.3% at 3.5 V. Moreover, the peak luminance of LEDs with sulfobetaine ligand exceeded 24000 cd/m^2.

The chemical composition of LHP-QDs has an impact on optical properties such as PLQY and PL decay lifetime. However, conventional synthetic route with hot-injection methods result in lead-rich composition LHP-QDs, which act as surface trap site. To overcome this issue, the halide-rich composition control by using lead oxide and ammonium halide has also been demonstrated to obtain high quality LHP-QDs (Fig. 4d).[67] The PLQY of LHP-QDs increases with increasing halide element component. In addition, the removing excess lead element from LHP-QDs surface is also effective approach to prevent a trap site.[68] The halide-rich LHP-QDs could be formed by addition of small amount of thiocyanate. The thiocyanate treatment improves the PLQY due to controlling chemical composition of LHP-QDs from Pb/Br ration of 1:2.7 to 1:3.0

(Fig. 4e).

5. Blue and red perovskite QD LEDs

The combination of two different anions, mix-halide anion LHP-QDs such as $CsPb(Cl/Br)_3$ and $CsPb(Br/I)_3$ can be complemented blue (ca. 430–490 nm) and red (ca. 550–650 nm) region in visible range by adjustment of mix-halide anion ratio.[22, 69-72] The mix-halide LHP-QDs are commonly prepared three routes, direst synthesis method, blend in LHP-QDs method, and anion exchange method using halide salts. For the direct synthesis method, two lead halide salts such as $PbCl_2$:$PbBr_2$ or $PbBr_2$:PbI_2 are used in synthesis step of hot-injection method, which can be easily tuned an optical properties by changing ratio of lead halide salts. On the other hand, post-treatment of synthesized LHP-QDs are also utilized for the form of mix-halide composition due to their high ionic conductive properties. The anion exchange method of LHP-QDs that the replacement halide anion from Br^- anion to Cl^- or I^- anion in LHP-QDs at room temperature demonstrated by Akkerman et al. using various halide salt precursors (ammonium-halides or metal-halide salts) or blended with LHP-QDs dispersion with different halide composition ($CsPbCl_3$:$CsPbBr_3$ or $CsPbBr_3$:$CsPbI_3$) (Fig. 5a).[69]

Blue $CsPb(Cl/Br)_3$ QDs based LEDs are still lower efficiency compared to the green $CsPbBr_3$ QD-LEDs. Song et al. have demonstrated blue $CsPb(Cl/Br)_3$ QD-LEDs with high luminance of 742 cd/m^2 and EQE of 0.07% with EL peak wavelength at 455 nm.[53] Blue $CsPb(Cl/Br)_3$ QDs coated with TMA was also reported with luminance of 8.7 cd/m^2 and peak emission at 480 nm.[60] Pan et al. have demonstrated the blue $CsPb(Cl/Br)_3$ by novle ligand-exchange process of with di-dodecyl dimethyl ammonium chloride (DDACl) to replace bromine anion by chloride anion.[63] Blue LED with DDAC capped $CsPb(Cl/Br)_3$ exhibited the EQE of 1.9% with EL peak at 490 nm. Thus, ligand exchange strategy enables to not only improve charge balance and efficiencies of LEDs, but also to control emission wavelength of LHP-QDs. Yao et al. have also reported the $CsPb(Cl/Br)_3$ by mixing method with directly synthesized $CsPbCl_3$ and $CsPbBr_3$ to obtain the blue emission at 470 nm with narrow FWHM of 15 nm.[73] The use of mix dispersion with hexane and toluene led to the smooth surface roughness and small grain size in film. In addition, nickel oxide was use as hole injection and transport layer to reduce hole injection barrier between $CsPb(Cl/Br)_3$ layer. The blue QD-LED with surface and energy level engineering reached a high luminance of 350 cd/m^2 with EQE of 0.07%. Further approach by using nafion perfluorinated ionomer (PFI) was reported to improve the green $CsPbBr_3$ QD[74] and blue $CsPb(Cl/Br)_3$ QD based LEDs[75]. The strong dipole effect of PFI could be controlled the energy level of under hole transport layer such as TFB (Fig. 5b). The blue $CsPb(Cl/Br)_3$ QD-LED with multilayer of TFB/PFI achieved a high luminance over 100 cd/m^2 and EQE of 0.5% with EL peak at 469 nm (Fig. 5c).

Red emission LHP-QDs are also required to for full color display applications. Therefore, mix

halides anion with $CsPb(Br/I)_3$ QDs and iodine based $CsPbI_3$ QDs have also demonstrated for red emission LEDs application.[76-78] In contrast to the blue $CsPb(Cl/Br)_3$ QD based LEDs, the efficiency of red QD-LEDs were comparable to the green $CsPbBr_3$ QD-LED. The red $CsPbI_3$ QDs with TMA based LED reached EQE of 5.7%, which was 10-fold higher than the untreated $CsPbI_3$ based LED.[60] Similarly, amine based aliphatic polymer polyethyleneamine (PEI) can be also served as a passivation layer of red $CsPb(Br/I)_3$ LHP-QDs, which led to considerably improvement PLQYs from 15% without PEI to 70% with PEI.[79] Moreover, PEI could be reduced the work function of metal oxides such as zinc oxide (ZnO) due to form the interfacial dipole moments.[80] The inverted red LEDs with multilayer structure of ZnO/PEI as a both passivation and electron injection layers exhibited a low-turn on voltage of 1.9 V and high EQE of up to 6.3%. Ligand exchange process with bidentate ligand based on double carboxylic groups, namely 2,2′-iminodibenzoic acid (IDA), have also demonstrated to passivate the surface of red $CsPbI_3$ QDs.[81] IDA-$CsPbI_3$ QDs exhibited a higher PLQY (95%) compared with untreated $CsPbI_3$ QDs (80%), although no significant change was observed in the crystal structure, PL emission, and absorption spectra. Whereas longer PL decay component was observed after IDA ligand exchange LHP-QDs due to less surface trap site by IDA capping (Fig. 5d, e). The double carboxylic groups is able to bind to two surface Pb atom, which is stronger binding energy (1.4 eV) than that of single carboxyl OA (1.14 eV). Thus, PL emission of IDA- $CsPbI_3$ QDs was stable even after 15 days, while untreated $CsPbI_3$ QDs exhibited PL quenching after only 5 day. The red LED based on IDA-$CsPbI_3$ QD has a peak EQE of 5.02%, which is 2-fold higher that of untreated $CsPbI_3$ QD based LED (2.26%).

The operational stability and color stability of LHP-QD LEDs still remain to be solved for their LED applications. In particular, mix halide anion based on $CsPb(Br/I)_3$ LEDs exhibited a red-shift of EL spectra under during operation, which suggesting the halide anion segregation effect.[82] The red-shifts of EL spectra hinges on the chemical composition of mix halide I/Br ratio. The LHP-QD LED with lower I/Br ratio (lower-iodide content) exhibited a large red-shift with shorter time compared to the LEDs with higher I/Br ratio (higher-iodide content) (Fig. 5f). Furthermore, similar color shift by anion segregation effect under applied electric field were observed in blue $CsPb(Cl/Br)_3$ LEDs.[75] In order to address this issue, further investigations are required for improvement operational stability and color stability of LHP-QD LEDs.

6. Summary and outlook

LHP-QDs based LEDs with high color purity emission spectra in the full visible range have been demonstrated as a good candidate for next-generation light-emitting materials in lighting and display applications over the past few years. One of the key feature of LHP-QDs is narrow FWHM emission, ~15 nm for blue, ~20 nm for green, and 30 nm for red, respectively, which are superior than those of conventional organic emitters (fluorescent and phosphorescent materials) or Cd-based core-shell QDs. Thus, their LHP-QDs emission spectra can be covered the wide color gamut BT.2020. LHP-QDs are consisted almost entirely of inorganic elements, the valence band and conduction band of LHP-QDs are similar to the HOMO or LUMO level of organic light-emitting materials, which lead to fabrication of device with similar structure of OLEDs.

In this review, we discussed the current approaches to achieve highly efficient LHP-QDs based LEDs, hot-injection synthesis method for LHP-QDs, purification process, ligand exchange approaches for surface passivation, and blue and red LHP-QD LEDs. In particular, the chemical composition of the LHP-QDs has a great influence on their optical properties. The precise control of A-site by mix cation strategy and reducing anion defect in X-site are needed in order to achieve both high PLQY of LHP-QDs film and high EQE of LEDs. The reprecipitation method by good (low dielectric constant) and poor (high dielectric) solvent is not ideal purification process because LHP-QDs are quite sensitive to high dielectric constant solvent such as alcohols. Thus, further investigation of low dielectric poor solvent or non reprecipitation purification process are significant and beneficial for high quality LHP-QDs. In addition, surface ligand admits some improvement due to electrical insulating property. The use of short alkyl ligand, aryl ligand, and inorganic ligand are needs to solve this issue.

The fabrication of LHP-QDs, energy level alignment between LHP-QDs and adjacent charge injection/transport layers is key feature to realize effective recombination in LHP-QDs emission layer. From this viewpoint, the analysis for valence band and conduction band of LHP-QDs in film by additional passivation layer or ligand exchange strategy are also needs. Moreover, LHP-QDs film is difficult to fabricate layer-by layer or multilayer structure by solution processing because LHP-QDs capped with conventional long alkyl ligand is easy soluble in coating solvent of upper layer. The fabrication of LHP-QDs LED is limited by hybrid solution and evaporation process so far. Therefore, further approaches to form insoluble LHP-QDs film are strongly desired for all solution processed multilayer structure and highly efficient LHP-QDs LEDs.

Acknowledgements

The authors acknowledge the Center of Innovation Program and and the Strategic Promotion of Innovative R&D Program of the Japan Science and Technology Agency (JST).

Biography of Authors

Takayuki Chiba is an assistant professor in the Graduate School of Organic Materials Science at Yamagata University, Japan. He received his Ph.D. in 2011 from the Department of Organic Device Engineering at Yamagata University. He was a post-doctoral fellow at Yamagata University in 2011-2014. His research is focused on perovskite QDs light-emitting devices.

Junji Kido is a full professor in the Graduate School of Organic Materials Science at Yamagata University. He received his Ph.D. in polymer chemistry from Poly- technic University, New York, in 1989. From 2003 to 2010, Kido served as the general director of the Research Institute for Organic Electronics founded by the government of Yamagata Prefecture. He invented white organic light-emitting devices in 1993 and is working on the development of high performance organic light-emitting devices.

Reference

1. Z. K. Tan, R. S. Moghaddam, M. L. Lai, P. Docampo, R. Higler, F. Deschler, M. Price, A. Sadhanala, L. M. Pazos, D. Credgington, F. Hanusch, T. Bein, H. J. Snaith and R. H. Friend, *Nat. nanotechnol.*, 2014, **9**, 687-692.
2. H. Cho, S. H. Jeong, M. H. Park, Y. H. Kim, C. Wolf, C. L. Lee, J. H. Heo, A. Sadhanala, N. Myoung, S. Yoo, S. H. Im, R. H. Friend and T. W. Lee, *Science*, 2015, **350**, 1222-1225.
3. J. Wang, N. Wang, Y. Jin, J. Si, Z. K. Tan, H. Du, L. Cheng, X. Dai, S. Bai, H. He, Z. Ye, M. L. Lai, R. H. Friend and W. Huang, *Adv. Mater.*, 2015, **27**, 2311-2316.
4. Y. H. Kim, H. Cho, J. H. Heo, T. S. Kim, N. Myoung, C. L. Lee, S. H. Im and T. W. Lee, *Adv. Mater.*, 2015, **27**, 1248-1254.
5. S. Kumar, J. Jagielski, N. Kallikounis, Y. H. Kim, C. Wolf, F. Jenny, T. Tian, C. J. Hofer, Y. C. Chiu, W. J. Stark, T. W. Lee and C. J. Shih, *Nano Lett.*, 2017, **17**, 5277-5284.
6. L. Meng, E. P. Yao, Z. R. Hong, H. J. Chen, P. Y. Sun, Z. L. Yang, G. Li and Y. Yang, *Adv. Mater.*, 2017, **29**, 1603826.
7. L. Q. Zhang, X. L. Yang, Q. Jiang, P. Y. Wang, Z. G. Yin, X. W. Zhang, H. R. Tan, Y. Yang, M. Y. Wei, B. R. Sutherland, E. H. Sargent and J. B. You, *Nat. Commun.*, 2017, **8**, 15640.
8. H. Cho, C. Wolf, J. S. Kim, H. J. Yun, J. S. Bae, H. Kim, J. M. Heo, S. Ahn and T. W. Lee, *Adv. Mater.*, 2017, **29**, 1700579.
9. C. Wu, Y. T. Zou, T. Wu, M. Y. Ban, V. Pecunia, Y. J. Han, Q. P. Liu, T. Song, S. Duhm and B. Q. Sun, *Adv. Funct. Mater.*, 2017, **27**, 1700338.
10. G. E. Eperon, T. Leijtens, K. A. Bush, R. Prasanna, T. Green, J. T. W. Wang, D. P. McMeekin, G. Volonakis, R. L. Milot, R. May, A. Palmstrom, D. J. Slotcavage, R. A. Belisle, J. B. Patel, E. S. Parrott, R. J. Sutton, W. Ma, F. Moghadam, B. Conings, A. Babayigit, H. G. Boyen, S. Bent, F. Giustino, L. M. Herz, M. B. Johnston, M. D. McGehee and H. J. Snaith, *Science*, 2016, **354**, 861-865.
11. Y. C. Zhao, J. Wei, H. Li, Y. Yan, W. K. Zhou, D. P. Yu and Q. Zhao, *Nat. Commun.*, 2016, **7**, 10228.
12. E. B. Bi, H. Chen, F. X. Xie, Y. Z. Wu, W. Chen, Y. J. Su, A. Islam, M. Gratzel, X. D. Yang and L. Y. Han, *Nat. Commun.*, 2017, **8**, 15330.
13. M. Era, S. Morimoto, T. Tsutsui and S. Saito, *Appl. Phys. Lett.*, 1994, **65**, 676-678.
14. Z. Xiao, R. A. Kerner, L. Zhao, N. L. Tran, K. M. Lee, T.-W. Koh, G. D. Scholes and B. P. Rand, *Nat. Photon.*, 2017, **11**, 108-115.
15. M. J. Yuan, L. N. Quan, R. Comin, G. Walters, R. Sabatini, O. Voznyy, S. Hoogland, Y. B. Zhao, E. M. Beauregard, P. Kanjanaboos, Z. H. Lu, D. H. Kim and E. H. Sargent, *Nat. nanotechnol.*, 2016, **11**, 872-877.
16. L. N. Quan, Y. B. A. Zhao, F. P. G. de Arquer, R. Sabatini, G. Walters, O. Voznyy, R. Comin,

Y. Y. Li, J. Z. Fan, H. R. Tan, J. Pan, M. J. Yuan, O. M. Bakr, Z. H. Lu, D. H. Kim and E. H. Sargent, *Nano Lett.*, 2017, **17**, 3701-3709.

17. X. L. Yang, X. W. Zhang, J. X. Deng, Z. M. Chu, Q. Jiang, J. H. Meng, P. Y. Wang, L. Q. Zhang, Z. G. Yin and J. B. You, *Nat. Commun.*, 2018, **9**, 1169.
18. S. T. Zhang, C. Yi, N. N. Wang, Y. Sun, W. Zou, Y. Q. Wei, Y. Cao, Y. F. Miao, R. Z. Li, Y. Yin, N. Zhao, J. P. Wang and W. Huang, *Adv. Mater.*, 2017, **29**, 1606600.
19. D. Han, M. Imran, M. Zhang, S. Chang, X.-g. Wu, X. Zhang, J. Tang, M. Wang, S. Ali, X. Li, G. Yu, J. Han, L. Wang, B. Zou and H. Zhon, *ACS Nano*, 2018, DOI: 10.1021/acsnano.8b05172.
20. N. N. Wang, L. Cheng, R. Ge, S. T. Zhang, Y. F. Miao, W. Zou, C. Yi, Y. Sun, Y. Cao, R. Yang, Y. Q. Wei, Q. Guo, Y. Ke, M. T. Yu, Y. Z. Jin, Y. Liu, Q. Q. Ding, D. W. Di, L. Yang, G. C. Xing, H. Tian, C. H. Jin, F. Gao, R. H. Friend, J. P. Wang and W. Huang, *Nat. Photon.*, 2016, **10**, 699-704.
21. L. Protesescu, S. Yakunin, M. I. Bodnarchuk, F. Krieg, R. Caputo, C. H. Hendon, R. X. Yang, A. Walsh and M. V. Kovalenko, *Nano Lett.*, 2015, **15**, 3692-3696.
22. G. Nedelcu, L. Protesescu, S. Yakunin, M. I. Bodnarchuk, M. J. Grotevent and M. V. Kovalenko, *Nano Lett.*, 2015, **15**, 5635-5640.
23. S. Yakunin, L. Protesescu, F. Krieg, M. I. Bodnarchuk, G. Nedelcu, M. Humer, G. De Luca, M. Fiebig, W. Heiss and M. V. Kovalenko, *Nat. Commun.*, 2015, **6**, 8056.
24. M. V. Kovalenko, L. Protesescu and M. I. Bodnarchuk, *Science*, 2017, **358**, 745-750.
25. H. Huang, M. I. Bodnarchuk, S. V. Kershaw, M. V. Kovalenko and A. L. Rogach, *ACS Energy Lett.*, 2017, **2**, 2071-2083.
26. Q. Shan, J. Song, Y. Zou, J. Li, L. Xu, J. Xue, Y. Dong, B. Han, J. Chen and H. Zeng, *Small*, 2017, **13**, 1701770.
27. Q. A. Akkerman, G. Raino, M. V. Kovalenko and L. Manna, *Nat. Mater*, 2018, **17**, 394-405.
28. S. A. Veldhuis, P. P. Boix, N. Yantara, M. J. Li, T. C. Sum, N. Mathews and S. G. Mhaisalkar, *Adv. Mater.*, 2016, **28**, 6804-6834.
29. F. Zhang, J. Song, B. Han, T. Fang and J. Z. Li, H., *Small methods*, 2018, 1700382.
30. Q. S. Shan, J. H. Li, J. Z. Song, Y. S. Zou, L. M. Xu, J. Xue, Y. H. Dong, C. X. Huo, J. W. Chen, B. N. Han and H. B. Zeng, *J. Mater. Chem. C*, 2017, **5**, 4565-4570.
31. A. Swarnkar, R. Chulliyil, V. K. Ravi, M. Irfanullah, A. Chowdhury and A. Nag, *Angew. Chem. Int. Edit.*, 2015, **54**, 15424-15428.
32. F. Zhang, H. Z. Zhong, C. Chen, X. G. Wu, X. M. Hu, H. L. Huang, J. B. Han, B. S. Zou and Y. P. Dong, *ACS Nano*, 2015, **9**, 4533-4542.
33. J. Xing, F. Yan, Y. W. Zhao, S. Chen, H. K. Yu, Q. Zhang, R. G. Zeng, H. V. Demir, X. W. Sun, A. Huan and Q. H. Xiong, *ACS Nano*, 2016, **10**, 6623-6630.

34. X. M. Li, Y. Wu, S. L. Zhang, B. Cai, Y. Gu, J. Z. Song and H. B. Zeng, *Adv. Funct. Mater.*, 2016, **26**, 2435-2445.
35. S. Wei, Y. C. Yang, X. J. Kang, L. Wang, L. J. Huang and D. C. Pan, *Chem. Commun.*, 2016, **52**, 7265-7268.
36. S. B. Sun, D. Yuan, Y. Xu, A. F. Wang and Z. T. Deng, *ACS Nano*, 2016, **10**, 3648-3657.
37. Z. Long, H. Ren, J. H. Sun, J. Ouyang and N. Na, *Chem. Commun.*, 2017, **53**, 9914-9917.
38. Q. Pan, H. C. Hu, Y. T. Zou, M. Chen, L. Z. Wu, D. Yang, X. L. Yuan, J. Fan, B. Q. Sun and Q. Zhang, *J. Mater. Chem. C*, 2017, **5**, 10947-10954.
39. H. W. Liu, Z. N. Wu, H. Gao, J. R. Shao, H. Y. Zou, D. Yao, Y. Liu, H. Zhang and B. Yang, *ACS Appl. Mater. Interfaces*, 2017, **9**, 42919-42927.
40. G. Almeida, L. Goldoni, Q. Akkerman, Z. Y. Dang, A. H. Khan, S. Marras, I. Moreels and L. Manna, *ACS Nano*, 2018, **12**, 1704-1711.
41. A. Z. Pan, B. He, X. Y. Fan, Z. K. Liu, J. J. Urban, A. P. Alivisatos, L. He and Y. Liu, *ACS Nano*, 2016, **10**, 7943-7954.
42. F. Giustino and H. J. Snaith, *ACS Energy Lett.*, 2016, **1**, 1233-1240.
43. T. C. Jellicoe, J. M. Richter, H. F. J. Glass, M. Tabachnyk, R. Brady, S. E. Dutton, A. Rao, R. H. Friend, D. Credgington, N. C. Greenham and M. L. Bohm, *J. Am. Chem. Soc.*, 2016, **138**, 2941-2944.
44. A. F. Wang, X. X. Yan, M. Zhang, S. B. Sun, M. Yang, W. Shen, X. Q. Pan, P. Wang and Z. T. Deng, *Chem. Mater.*, 2016, **28**, 8132-8140.
45. D. Parobek, B. J. Roman, Y. T. Dong, H. Jin, E. Lee, M. Sheldon and D. H. Son, *Nano Lett.*, 2016, **16**, 7376-7380.
46. W. van der Stam, J. J. Geuchies, T. Altantzis, K. H. W. van den Bos, J. D. Meeldijk, S. Van Aert, S. Bals, D. Vanmaekelbergh and C. D. Donega, *J. Am. Chem. Soc.*, 2017, **139**, 4087-4097.
47. J. Zhang, Y. Yang, H. Deng, U. Farooq, X. K. Yang, J. Khan, J. Tang and H. S. Song, *ACS Nano*, 2017, **11**, 9294-9302.
48. M. Y. Leng, Z. W. Chen, Y. Yang, Z. Li, K. Zeng, K. H. Li, G. D. Niu, Y. S. He, Q. C. Zhou and J. Tang, *Angew. Chem. Int. Edit.*, 2016, **55**, 15012-15016.
49. B. Yang, J. S. Chen, F. Hong, X. Mao, K. B. Zheng, S. Q. Yang, Y. J. Li, T. Pullerits, W. Q. Deng and K. L. Han, *Angew. Chem. Int. Edit.*, 2017, **56**, 12471-12475.
50. X. Y. Li, Y. B. Zhao, F. J. Fan, L. Levina, M. Liu, R. Quintero-Bermudez, X. W. Gong, L. N. Quan, J. Z. Fan, Z. Y. Yang, S. Hoogland, O. Voznyy, Z. H. Lu and E. H. Sargent, *Nat. Photon.*, 2018, **12**, 159-164.
51. Y. X. Yang, Y. Zheng, W. R. Cao, A. Titov, J. Hyvonen, J. R. Manders, J. G. Xue, P. H. Holloway and L. Qian, *Nat. Photon.*, 2015, **9**, 259-266.

52. H. B. Shen, W. R. Cao, N. T. Shewmon, C. C. Yang, L. S. Li and J. G. Xue, *Nano Lett.*, 2015, **15**, 1211-1216.
53. J. Song, J. Li, X. Li, L. Xu, Y. Dong and H. Zeng, *Adv. Mater.*, 2015, **27**, 7162-7167.
54. H. L. Huang, F. C. Zhao, L. G. Liu, F. Zhang, X. G. Wu, L. J. Shi, B. S. Zou, Q. B. Pei and H. Z. Zhong, *ACS Appl. Mater. Interfaces*, 2015, **7**, 28128-28133.
55. J. De Roo, M. Ibanez, P. Geiregat, G. Nedelcu, W. Walravens, J. Maes, J. C. Martins, I. Van Driessche, M. V. Kovalenko and Z. Hens, *ACS Nano*, 2016, **10**, 2071-2081.
56. V. K. Ravi, P. K. Santra, N. Joshi, J. Chugh, S. K. Singh, H. Rensmo, P. Ghosh and A. Nag, *Journal of Physical Chemistry Letters*, 2017, **8**, 4988-4994.
57. T. Chiba, K. Hoshi, Y. J. Pu, Y. Takeda, Y. Hayashi, S. Ohisa, S. Kawata and J. Kido, *ACS Appl. Mater. Interfaces*, 2017, **9**, 18054-18060.
58. K. Hoshi, T. Chiba, J. Sato, Y. Hayashi, Y. Takahashi, H. Ebe, S. Ohisa and J. Kido, *ACS Appl. Mater. Interfaces*, 2018, **10**, 24607-24612.
59. J. Li, L. Xu, T. Wang, J. Song, J. Chen, J. Xue, Y. Dong, B. Cai, Q. Shan, B. Han and H. Zeng, *Adv. Mater.*, 2017, **29**, 1603885.
60. G. Li, F. W. Rivarola, N. J. Davis, S. Bai, T. C. Jellicoe, F. de la Pena, S. Hou, C. Ducati, F. Gao, R. H. Friend, N. C. Greenham and Z. K. Tan, *Adv. Mater.*, 2016, **28**, 3528-3534.
61. H. Huang, H. Lin, S. V. Kershaw, A. S. Susha, W. C. H. Choy and A. L. Rogach, *Journal of Physical Chemistry Letters*, 2016, **7**, 4398-4404.
62. J. Pan, S. P. Sarmah, B. Murali, I. Dursun, W. Peng, M. R. Parida, J. Liu, L. Sinatra, N. Alyami, C. Zhao, E. Alarousu, T. K. Ng, B. S. Ooi, O. M. Bakr and O. F. Mohammed, *J. Phys. Chem. Lett.*, 2015, **6**, 5027-5033.
63. J. Pan, L. N. Quan, Y. Zhao, W. Peng, B. Murali, S. P. Sarmah, M. Yuan, L. Sinatra, N. M. Alyami, J. Liu, E. Yassitepe, Z. Yang, O. Voznyy, R. Comin, M. N. Hedhili, O. F. Mohammed, Z. H. Lu, D. H. Kim, E. H. Sargent and O. M. Bakr, *Adv. Mater.*, 2016, **28**, 8718-8725.
64. J. Z. Song, J. H. Li, L. M. Xu, J. H. Li, F. J. Zhang, B. N. Han, Q. S. Shan and H. B. Zeng, *Adv. Mater.*, 2018, **30**, 1800764.
65. Y. S. Tan, Y. T. Zou, L. Z. Wu, Q. Huang, D. Yang, M. Chen, M. Y. Ban, C. Wu, T. Wu, S. Bai, T. Song, Q. Zhang and B. Q. Sun, *ACS Appl. Mater. Interfaces*, 2018, **10**, 3784-3792.
66. F. Krieg, S. T. Ochsenbein, S. Yakunin, S. ten Brinck, P. Aellen, A. Suess, B. Clerc, D. Guggisberg, O. Nazarenko, Y. Shynkarenko, S. Kumar, C. J. Shih, I. Infante and M. V. Kovalenko, *ACS Energy Lett.*, 2018, **3**, 641-646.
67. P. Z. Liu, W. Chen, W. G. Wang, B. Xu, D. Wu, J. J. Hao, W. Y. Cao, F. Fang, Y. Li, Y. Y. Zeng, R. K. Pan, S. M. Chen, W. Q. Cao, X. W. Sun and K. Wane, *Chem. Mater.*, 2017, **29**, 5168-5173.

68. B. A. Koscher, J. K. Swabeck, N. D. Bronstein and A. P. Alivisatos, *J. Am. Chem. Soc.*, 2017, **139**, 6566-6569.
69. Q. A. Akkerman, V. D'Innocenzo, S. Accornero, A. Scarpellini, A. Petrozza, M. Prato and L. Manna, *J. Am. Chem. Soc.*, 2015, **137**, 10276-10281.
70. P. Ramasamy, D. H. Lim, B. Kim, S. H. Lee, M. S. Lee and J. S. Lee, *Chem. Commun.*, 2016, **52**, 2067-2070.
71. C. Guhrenz, A. Benad, C. Ziegler, D. Haubold, N. Gaponik and A. Eychmuller, *Chem. Mater.*, 2016, **28**, 9033-9040.
72. N. J. L. K. Davis, F. J. De la Pena, M. Tabachnyk, J. M. Richter, R. D. Lamboll, E. P. Booker, F. W. R. Rivarola, J. T. Griffiths, C. Ducati, S. M. Menke, F. Deschler and N. C. Greenham, *J. Phys. Chem. C*, 2017, **121**, 3790-3796.
73. E. P. Yao, Z. L. Yang, L. Meng, P. Y. Sun, S. Q. Dong, Y. Yang and Y. Yang, *Adv. Mater.*, 2017, **29**, 1606859.
74. X. Zhang, H. Lin, H. Huang, C. Reckmeier, Y. Zhang, W. C. Choy and A. L. Rogach, *Nano Lett.*, 2016, **16**, 1415-1420.
75. M. K. Gangishetty, S. C. Hou, Q. M. Quan and D. N. Congreve, *Adv. Mater.*, 2018, **30**, 1706226.
76. A. Swarnkar, A. R. Marshall, E. M. Sanehira, B. D. Chernomordik, D. T. Moore, J. A. Christians, T. Chakrabarti and J. M. Luther, *Science*, 2016, **354**, 92-95.
77. C. Zou, C. Y. Huang, E. M. Sanehira, J. M. Luther and L. Y. Lin, *Nanotechnology*, 2017, **28**, 455201.
78. F. Liu, Y. H. Zhang, C. Ding, S. Kobayashi, T. Izuishi, N. Nakazawa, T. Toyoda, T. Ohta, S. Hayase, T. Minemoto, K. Yoshino, S. Y. Dai and Q. Shen, *ACS Nano*, 2017, **11**, 10373-10383.
79. X. Zhang, C. Sun, Y. Zhang, H. Wu, C. Ji, Y. Chuai, P. Wang, S. Wen, C. Zhang and W. W. Yu, *J. Phys. Chem. Lett.*, 2016, **7**, 4602-4610.
80. Y. Zhou, C. Fuentes-Hernandez, J. Shim, J. Meyer, A. J. Giordano, H. Li, P. Winget, T. Papadopoulos, H. Cheun, J. Kim, M. Fenoll, A. Dindar, W. Haske, E. Najafabadi, T. M. Khan, H. Sojoudi, S. Barlow, S. Graham, J. L. Bredas, S. R. Marder, A. Kahn and B. Kippelen, *Science*, 2012, **336**, 327-332.
81. J. Pan, Y. Q. Shang, J. Yin, M. De Bastiani, W. Peng, I. Dursun, L. Sinatra, A. M. El-Zohry, M. N. Hedhili, A. H. Emwas, O. F. Mohammed, Z. J. Ning and O. M. Bakr, *J. Am. Chem. Soc.*, 2018, **140**, 562-565.
82. P. Vashishtha and J. E. Halpert, *Chem. Mater.*, 2017, **29**, 5965-5973.

Figure caption

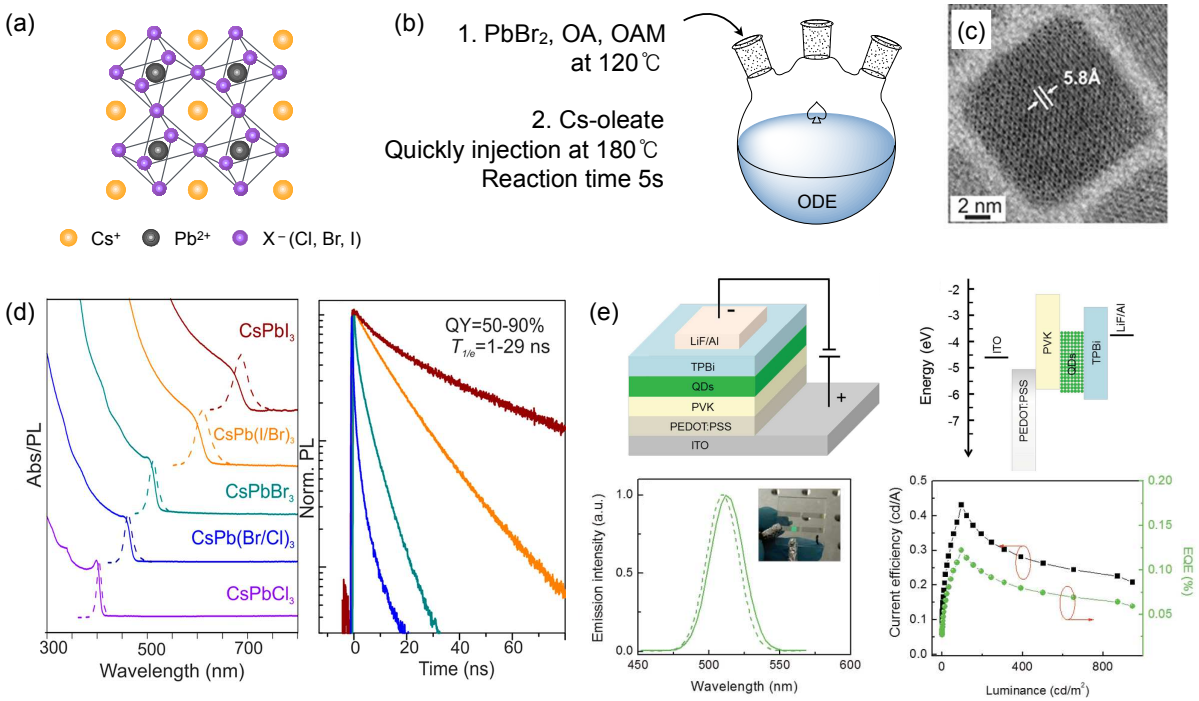

Fig. 1 (a) Schematic of the $CsPbX_3$ QDs structure. (b) Schematic of the LHP-QDs synthesis by hot-injection method. (c) TEM image of $CsPbBr_3$ QDs and (d) Absorption, PL and PL decay curves of LHP-QDs. Reprinted with permission from ref. 21. Copyright. (e) Device structure, energy level diagram, EL spectra, and current efficiency and EQE of LHP-QD LED. Reprinted with permission from ref. 53.

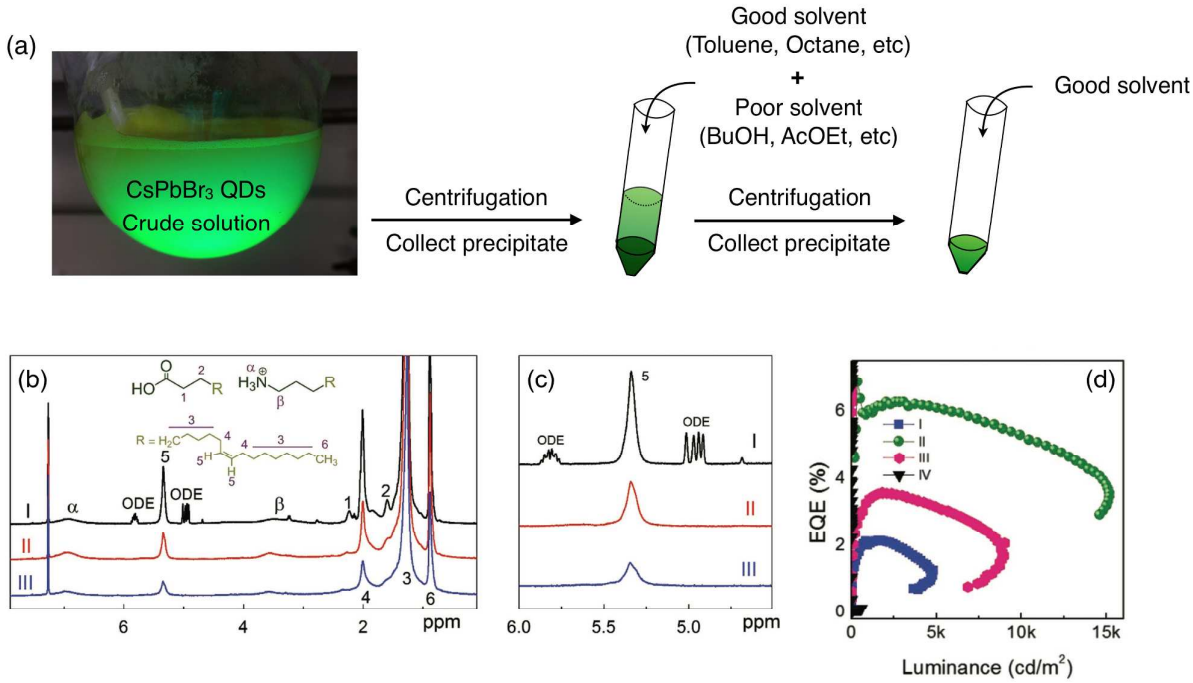

Fig. 2 (a) Schematic overview of the LHP-QD purification process with reprecipitation method. (b, c) ^{1}H-NMR spectra of $CsPbBr_3$ with different washing cycle. (d) EQE curves of $CsPbBr_3$ QDs based LEDs. Reprinted with permission from ref. 59.

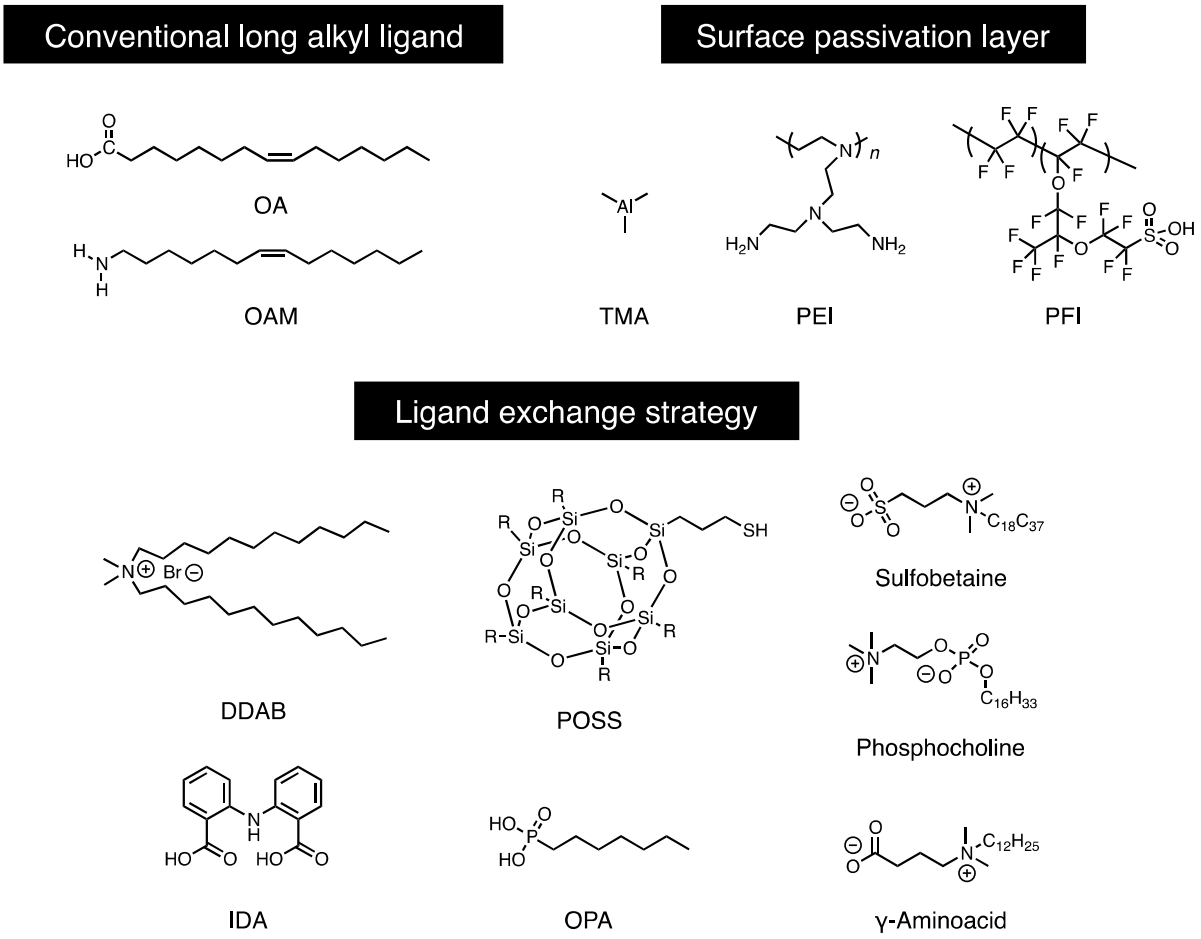

Fig.3 Chemical structure of conventional alkyl ligand, surface passivation layer, and alternative ligands.

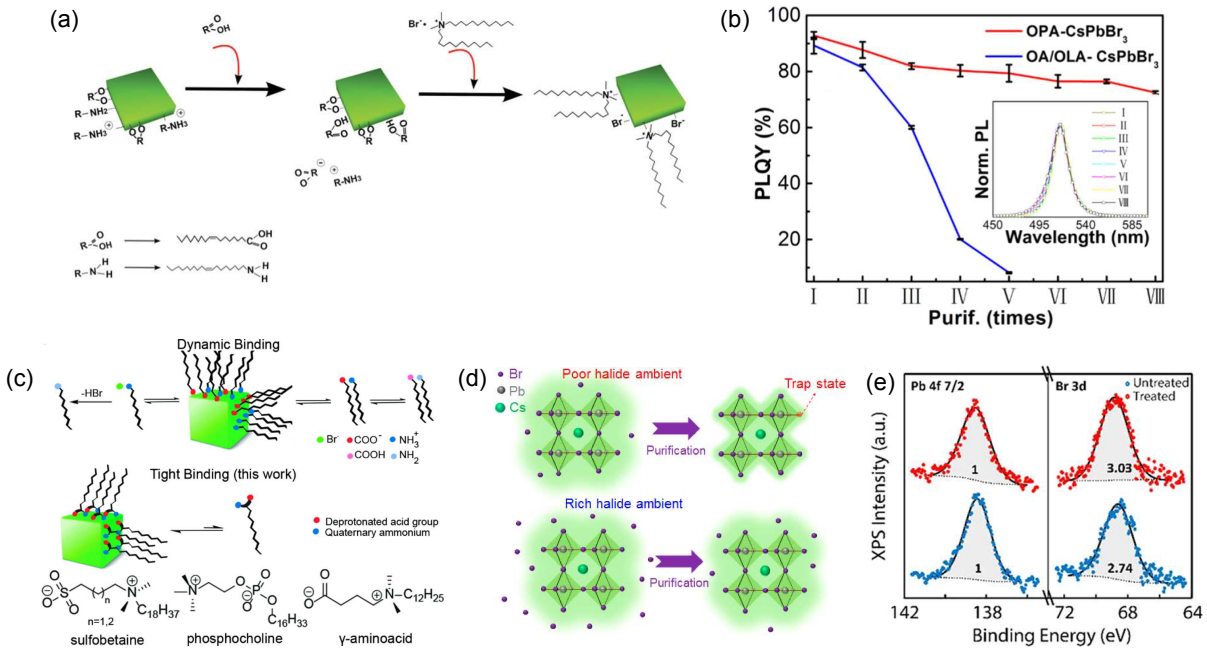

Fig.4 (a) Schematic of the ligand exchange on LHP-QD with DDAB. Reprinted with permission from ref. 63. (b) PLQY of OPA capped $CsPbBr_3$ with different washing cycle. Reprinted with permission from ref. 65. Copyright. (c) Schematic of the ligand desorbing and binding to LHP-QDs. Reprinted with permission from ref. 66. (d) Schematic of halide-poor and halide-rich composition for synthesis for LHP-QDs. Reprinted with permission from ref. 67. (e) XPS spectra of the Pb 4f7/2 and Br 3d for the untreated and thiocyanate□ treated LHP-QDs. Reprinted with permission from ref. 68.

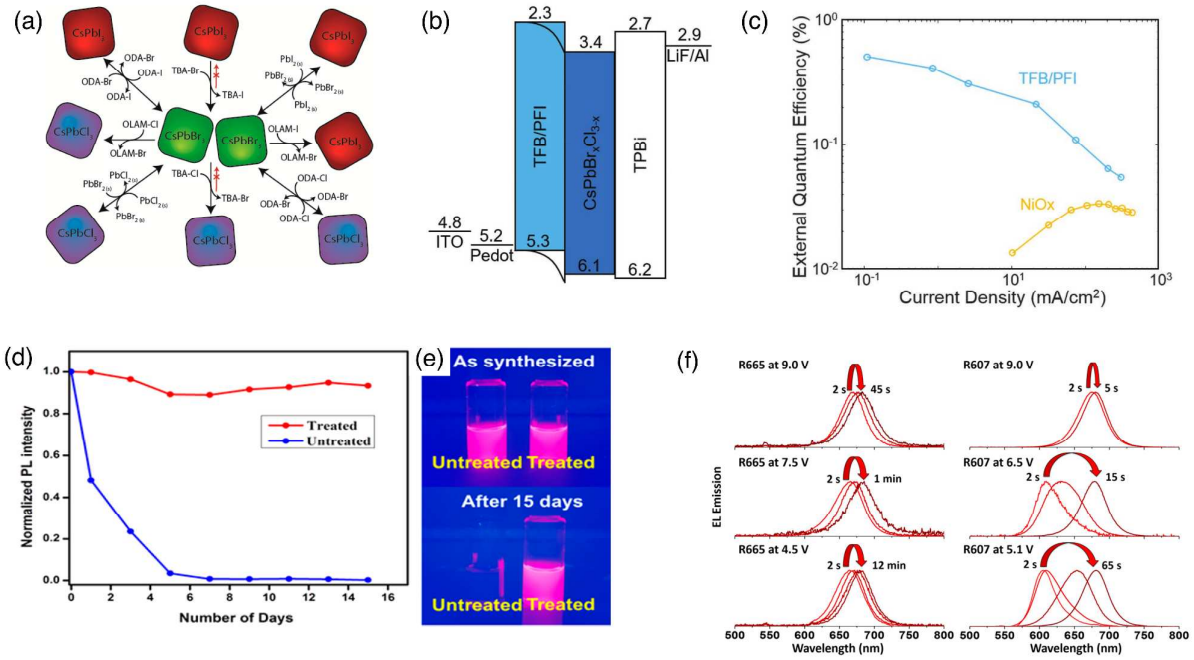

Fig. 5 (a) Schematic overview of the anion exchange reaction on $CsPbX_3$ QDs with different precursors. Reprinted with permission from ref. 69. (b) Energy diagram and (c) EQE curves of blue $CsPb(Cl/Br)_3$ based LED. Reprinted with permission from ref. 75. (d) PLQY and (e) photograph as a function of days for IDA-capped LHP-QDs and untreated LHP-QDs aged for 15 days. Reprinted with permission from ref. 81. (f) EL peak shift of higher-iodide content and lower-iodide content $CsPb(Br/I)_3$ based LEDs at different voltage. Reprinted with permission from ref. 82.

Table of contents